# Comparing SNR Benefits between Single-Mask Edge-Illumination and Free-Space Propagation X-ray Phase Contrast Imaging

Jingcheng Yuan<sup>a</sup>, Ian Harmon<sup>a</sup>, and Mini Das<sup>a,b,\*</sup>

<sup>a</sup>Department of Physics, University of Houston, Houston 77204, USA <sup>b</sup>Department of Biomedical Engineering, University of Houston, Houston 77204, USA

## ABSTRACT

X-ray phase contrast imaging (PCI) has a great potential for improving the visibility of soft tissues in medical imaging. Single-mask edge-illumination (EI) (also sometime referred to as coded-aperture) phase contrast imaging method has been developed with the ability to obtain differential phase contrast with simpler experimental setup in comparison to grating based or conventional double mask EI PCI. We show results of single-mask PCI and results of differential phase contrast estimation in a single shot. The potential of this single mask PCI to reduce the radiation dose and improved contrast has not been fully investigated yet. In this work we compared the x-ray dose requirement of single-mask method with other methods by analyzing the SNR under different level of detector counts. We also propose and demonstrate a new model based on TIE for differential retrieval from single mask EI PCI with experimental data.

**Keywords:** X-ray phase contrast imaging, edge-illumination, coded aperture, single-mask, single-shot retrieval

## 1. INTRODUCTION

X-ray projection imaging, utilizing the difference of attenuation property within the measured object, is commonly used for medical imaging of the human body. However, there are limitations for absorption-based x-ray images because the attenuation value of low-atomic-number materials, soft tissue, for example, is relatively low. In addition, the contrast between different features of soft tissue is very low, for example, between normal tissue and lesion/cancers. X-ray phase-contrast imaging (PCI) is being investigated for the potential of inherently increasing the contrast of signal detection for soft tissues without contrast agents. The technique of PCI with single-shot measurement, high contrast and low radiation dose have attracted particular interest.

The simplest method to achieve x-ray phase contrast imaging is free-space propagation method,<sup>1</sup> which does not require any optics in the beam path, but only increase the object-to-detector distance. Due to the x-ray refraction by the object, the distribution of x-ray intensity on the detector plane will be changed, resulting in edge enhancement for most materials (Fig. 1), which can be modeled by the approximation form of transport-of-intensity equation (TIE):

$$I(z, \vec{r}) = I(0, \vec{r}) - \frac{z}{k} I(0, \vec{r}) \nabla_{\perp}^2 \phi(\vec{r})$$

$$\tag{1}$$

where  $I(z, \vec{r})$  and  $I(0, \vec{r})$  is the x-ray intensity on the object plane and detector plane respectively, z is the object-to detector distance.

A new method known as single-mask edge-illumination method for PCI was developed by Krejci et al,<sup>2</sup> which is similar with propagation-based method but adding a periodic absorption mask closely upstream the object. SM method can provide two different images in a single shot: one is phase contrast image similar with FSP method, the other is differential phase contrast (DPC) image which provide the information of the gradient of phase distribution. In this paper, we show the comparison between FSP and SM method with a potential for contrast enhancement, image quality and dose reduction.

Further author information: (Send correspondence to MD)

M. D. .: E-mail: mdas@uh.edu

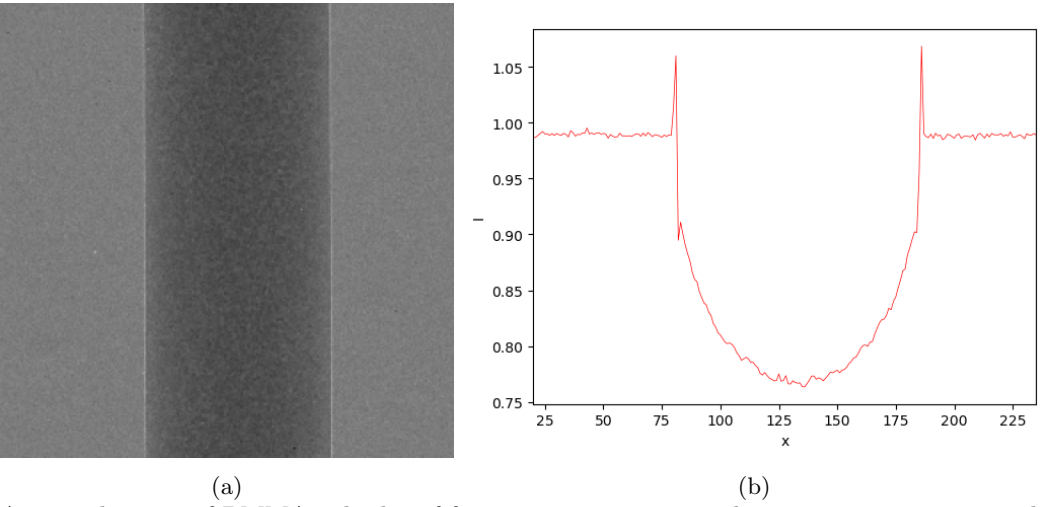


Figure 1: A typical image of PMMA cylinder of free-space propagation phase contrast imaging and its average cross-section profile.

The schematic of the imaging geometry is shown in Fig. 2. The period of the mask is twice of the detector pitch after magnification, creating a set of small strip-like beams of x-ray. The mask strips are aligned parallel to the detector columns and the beamlets aligned with detector pixels. In the absence of an object in the beam path, the intensity measured by the pixels are expected to be homogeneous. When the object is introduced, the refractive effects results in beam shifting causing variations that can then be measured directly. These variations are directly proportional to the distribution of refraction index within the object. These measurements are now possible without a very high resolution detector.<sup>3</sup> The refraction angle is proportional to the gradient of phase and can be analyzed by examining intensity variations between pixels:

$$\Delta\theta_x = \frac{1}{k} \frac{\partial\phi}{\partial x} \tag{2}$$

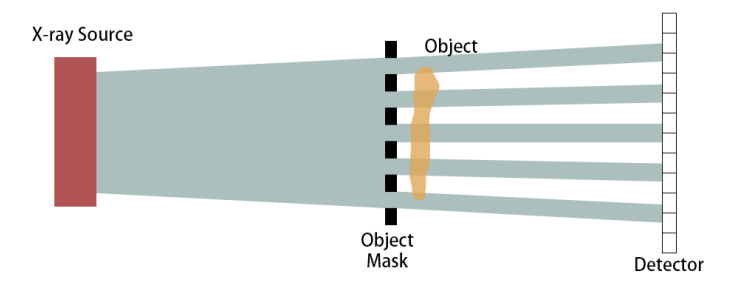


Figure 2: Schematic of single-mask edge-illumination setup.

# 2. THEORY

## 2.1 Theoretic Model

Our theoretic model for single-mask PCI started with general transport-of-intensity-equation (TIE):

$$I(z, \vec{r}) = I(0, \vec{r}) - \frac{z}{k} (\nabla_{\perp} I(0, \vec{r}) \cdot \nabla_{\perp} \phi(\vec{r}) + I(0, \vec{r}) \nabla_{\perp}^{2} \phi(\vec{r}))$$

$$(3)$$

where  $I(0, \vec{r}) = T(\vec{r}) \cdot M(x)$ .  $T(\vec{r})$  and M(x) is the transmission function of the object and the mask, respectively. Therefore:

$$\nabla_{\perp} I(0, \vec{r}) = T \nabla_{\perp} M + M \nabla_{\perp} T \approx T \partial_x M \tag{4}$$

Similar to our previous model,  $^{4,5}$  integrating Equation (3) over the  $n^{th}$  detector pixel, we get:

$$I_n = wT_n(1 - L_n) + (-1)^n T_n D_n$$
(5)

where  $L_n = \frac{z}{k} \nabla_{\perp}^2 \phi(x_n)$ ,  $D_n = \frac{z}{k} \partial_x \phi(x_n)$ , w is the effective pixel width, and  $\phi(x_n)$  is the phase change at the  $n^{th}$  pixel.

The first term of Equation (5), which we call FSP term, has the same form with Equation (1) but decreased by multiplying the effective pixel width; the second term contains the information of DPC, so we call it DPC term. We also need to take an image without any object and use this image as the flat-field image to do flat-field corrections. We can get the following result:

$$I_n = \frac{I_{object+mask}}{I_{mask-only}} = T_n(1 - L_n) + \frac{(-1)^n}{w} T_n D_n$$
(6)

## 2.2 Retrieval Method

To separate the FSP term and the DPC term, we examine intensity variations between pixels and arrive at solutions based on the transport models. From the models we understand that the Laplacian term is negligible and this is used in the solutions to retrieved FSP image and is the DPC image.

## 3. METHODS

# 3.1 Imaging System

We used a poly-chromatic micro-focus x-ray tube (Hama-matsu L8121-03) operating with a focal spot of 7 m. The tube voltage and current were 40 kV and 240 A respectively. The source to object and object to detector distance were both 60 cm. We used the gold mask (167-200 microns thick gold strips on a 525 microns Si plus 3m Ti substrate) manufactured by Microworks. All the presented data was collected using a Silicon Medipix3 detector with 55 micron pixel pitch under charge summing mode.

To verify the accuracy of the method, the phantom we used was a PMMA rod (3 mm in diameter). For comparison, both FSP method and SM method are measured under same experimental settings. Both methods are measured under different detector counts.

## 3.2 Simulation Method

Our simulation method is based on Monte-Carlo method. In our simulation, we randomly generates a large number of photons with different energy and different position near the focal spot of x-ray source. The spectrum of photon energy is based on TASMIP spectra calculator, and the position of photons have a 2D Gaussian distribution corresponding to the focal spot size of the x-ray source. Each photon hits on a random position at the object plane. The thickness map and material of the mask and the object are the same with our experiment. The probability of each photon passing through the object and the mask is calculated from the attenuation value. The refraction angle is calculated from (2). Based on the above, the position where each photon hits on the detector plane can be calculated. Finally, the photon number on each detector pixel is counted.

## 3.3 SNR Measurement

The SNR was calculated for each level of detector counts using the equation below:

$$SNR = \frac{I_{max} - I_{min}}{2\sigma_{BG}} \tag{7}$$

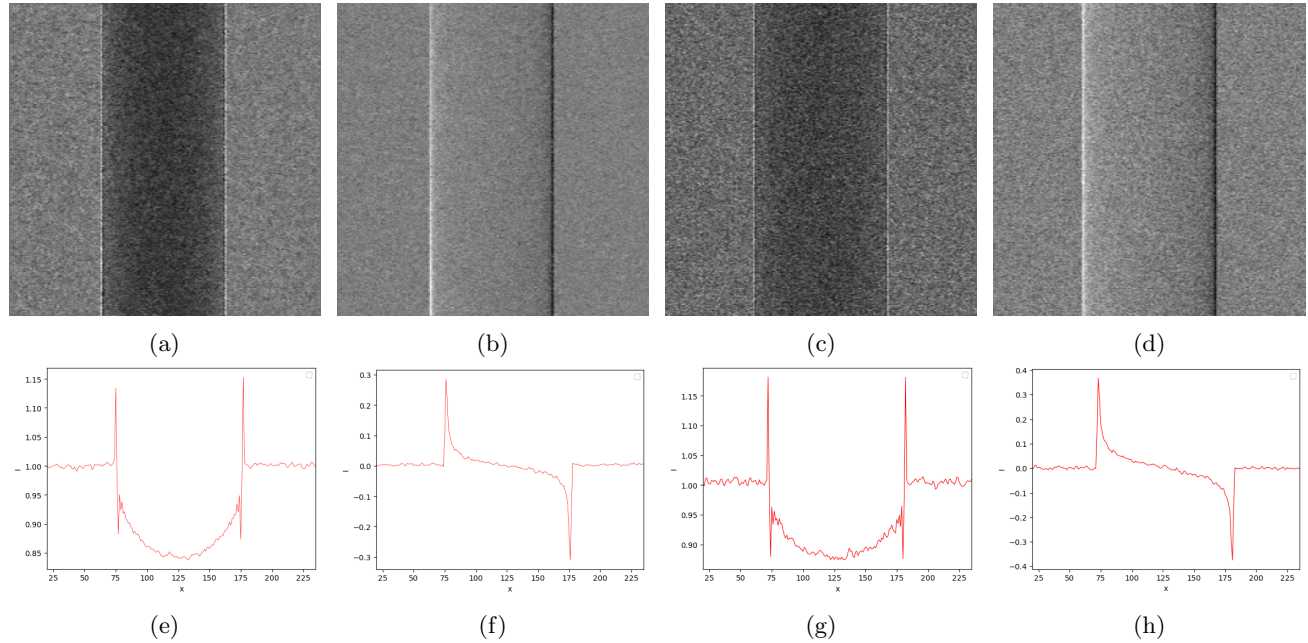


Figure 3: Result of simulation and experiment for single-mask method and their average cross-section profile.(a) retrieved FSP image from simulation data; (b) retrieved DPC image from simulation data; (c) retrieved FSP image from experiment data; (d) retrieved DPC image from experiment data; (e)-(h) average profile of (a)-(d).

where  $I_{max}$  and  $I_{min}$  are maximum and minimum values of average cross-section profile within ROI,  $\sigma_{BG}$  is the standard deviation in background region.

We select different ROI to calculate different types of signal. For the SNR of attenuation contrast, the ROI does not include the edge of the sample to avoid the effect of phase contrast signal on the edge. For the SNR of phase contrast image, including both FSP PCI and DPC image, the edge is included in ROI instead.

## 4. RESULTS

Fig. 3 shows the image of single-mask method from both experiment and simulation, as well as the average cross-section profile of each image. The images are taken under the same experimental geometry with images in Fig. 1. We could see that the FSP image retrieved from single -mask method is very similar to the image from FSP method but with a higher peak on the edge. The DPC images retrieved from single-mask method have a much higher contrast comparing with FSP images. Also we can notice the contrast of DPC image is maximum on the edge, which can enhance the visibility of the sample.

The main difference between simulation and experiment result is the signal intensity of simulation is stronger than experiment. This can be caused by many factors, for example, the signal intensity of experiment result can be affected by charge sharing effect because most of the photons hit on the small area close to the boundary of two pixels. Also the imperfection of the mask due to manufacture and the imperfect alignment of the mask can also reduce the signal intensity, which is hard to simulate.

Fig. 4 shows the comparison of simulation and experiment result with three different x-ray focal spot sizes. We could see both simulation and experiment results showed that with larger x-ray focal spot, the contrast of DPC image decrease significantly, which is within our expectation because a larger x-ray focal spot will cause blur on mask pattern on detector plane reducing the sensitivity required to capture refraction effects.

Fig. 5 shows the plot of SNR and detector counts. We notice a significant improvement of SNR from DPC image. For the same level of SNR, single-mask method can reduce the detector counts or x-ray dose for nearly 2.5 times compared with FSP method.

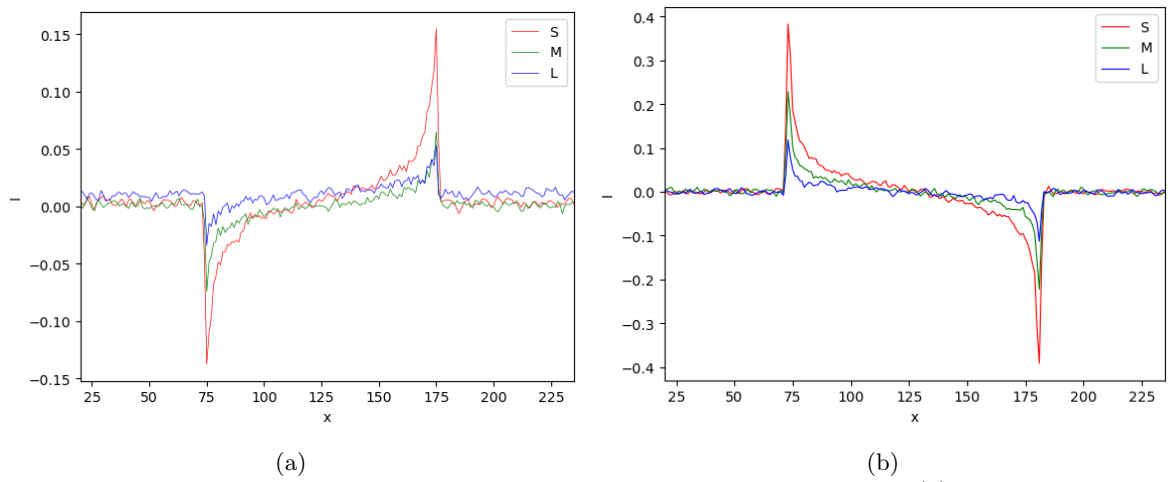


Figure 4: Average cross-section profile of DPC image with different focal spot.(a) Experiment result; (b) simulation result.

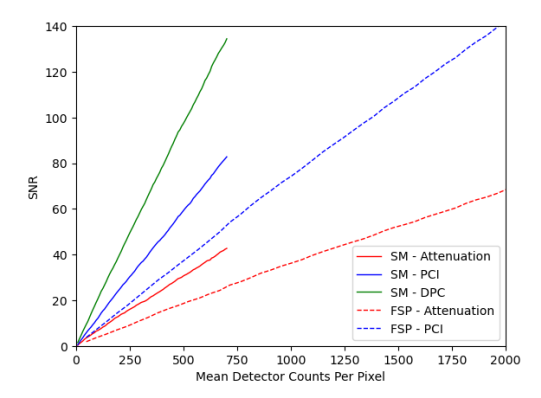


Figure 5: The SNR in different level of detector count numbers. Solid lines: result of single-mask method. Dashed lines: result of free-space propagation method. Red lines: SNR of attenuation image. Blue solid lines: SNR of FSP term of single-mask method. Blue dashed lines: SNR of FSP image. Green lines: SNR of differential phase contrast (DPC) image. results show significant improvement in SNR due to retrieved DPC.

# 5. CONCLUSION

In this work, we used our TIE model to derive a new retrieval method for single-mask edge-illumination phase contrast imaging. Our retrieval result shows that we can separate the FSP signal and the DPC signal from the raw image with good image quality.

We also used the same imaging system geometry to compare the SNR of free-space propagation PCI method and single-mask edge-illumination PCI method with different levels of detector counts. Our results demonstrate that the single-mask method can significantly reduce the level of detector counts, which corresponds to x-ray dose on the sample, for a certain SNR requirement.

# 6. ACKNOWLEDGEMENTS

This work was partially supported by funding from the NIH National Institute of Biomedical Imaging and Bioengineering (NIBIB) grant R01 EB EB029761, US Department of Defense (DOD) Congressionally Directed Medical Research Program (CDMRP) Breakthrough Award BC151607 and the National Science Foundation CAREER Award 1652892.

## REFERENCES

- [1] Wilkins, S. W., Gureyev, T. E., Gao, D., Pogany, A., and Stevenson, A. W., "Phase-contrast imaging using polychromatic hard X-rays," *Nature* **384**, 335–338 (Nov. 1996). Bandiera\_abtest: a Cg\_type: Nature Research Journals Number: 6607 Primary\_atype: Research Publisher: Nature Publishing Group.
- [2] Krejci, F., Jakubek, J., and Kroupa, M., "Hard x-ray phase contrast imaging using single absorption grating and hybrid semiconductor pixel detector," *Review of Scientific Instruments* 81(11), 113702 (2010).
- [3] Kallon, G. K., Vittoria, F. A., Endrizzi, M., Diemoz, P. C., Hagen, C. K., Zamir, A., Basta, D., and Olivo, A., "Detector requirements for single mask edge illumination x-ray phase contrast imaging applications," arXiv:1709.09005 [physics] (Sept. 2017). arXiv: 1709.09005.
- [4] Das, M. and Liang, Z., "Approximated transport-of-intensity equation for coded-aperture x-ray phase-contrast imaging," *Optics Letters* **39**, 5395–5398 (Sept. 2014). Publisher: Optica Publishing Group.
- [5] Das, M. and Liang, Z., "Spectral x-ray phase contrast imaging for single-shot retrieval of absorption, phase, and differential-phase imagery," *Opt. Lett.* **39**, 6343–6346 (Nov 2014).
- [6] Kallon, G. K., Diemoz, P. C., Vittoria, F. A., Basta, D., Endrizzi, M., and Olivo, A., "Comparing signal intensity and refraction sensitivity of double and single mask edge illumination lab-based x-ray phase contrast imaging set-ups," *Journal of Physics D: Applied Physics* 50, 415401 (sep 2017).
- [7] Vazquez, I., Harmon, I. E., Luna, J. C. R., and Das, M., "Quantitative phase retrieval with low photon counts using an energy resolving quantum detector," *Journal of the Optical Society of America A* 38, 71 (Jan. 2021).